ALT 12
Advanced Laser Technologies
2 – 6 September 2012, Thun, Switzerland

ALT 12
c/o Bern University of Applied Sciences
Engineering and Information Technology
Pestalozzistrasse 20, CH-3400 Burgdorf
info@alt12.org, www.alt12.org
0041 (0) 34 426 42 06

MECHANISM OF FEMTOSECOND LASER NANO-ABLATION FOR METALS

Authors:

M. Hashida, Y. Miyasaka, M. Shimizu, T. Ogata, H. Sakagami, S. Tokita, S. Sakabe

DOI: 10.12684/alt.1.45

Corresponding author: M. Hashida

e-mail: hashida@laser.kuicr.kyoto-u.ac.jp

Mechanism of femtosecond laser nano-ablation for metals

M. Hashida[1,2], Y. Miyasaka[1,2], M. Shimizu[1,2], T. Ogata[3], H. Sakagami[3,4], S. Tokita[1,2], S. Sakabe[1,2]

[1]Institute for Chemical Research, Kyoto University, Gokasho, Uji, 611-0011, Japan
[2]Department of Physics, Kyoto University, Kitashirakawa, Sakyo, 606-7501, Japan
[3]Department of Physics, Nagoya University, Nagoya, Aichi, 464-8602, Japan
[4]National Institute for Fusion Science, Toki-City, Gifu, 509-5292, Japan

Abstract

Metals have three ablation threshold fluences (high, middle and low-threshold fluence, here called) for femtosecond laser pulses. In order to investigate the physics of metal ablation under an intense optical field, the ions emitted from a laser-irradiated copper surface were studied by time-of-flight energy spectroscopy. The low laser fluence at which ions are emitted, $F_{th,L}$ is 0.028 J/cm^2, and two higher emission thresholds were identified at fluences of $F_{th,M}$ =0.195 J/cm^2 and $F_{th,H}$ =0.470 J/cm^2. The relation between the number of emitted ions per pulse N_i and laser fluence F was in good agreement with $N_i \propto F^4$ for $F_{th,L}$ - $F_{th,M}$, $N_i \propto F^3$ for $F_{th,M}$ - $F_{th,H}$, and $N_i \propto F^2$ for $\geq F_{th,H}$. The dependence of ion production on laser energy fluence is explained well by multiphoton absorption and optical field ionization.
For fluence levels near the middle to high ablation threshold, the formation of grating structures on metal surfaces has been observed. The interspaces of grating structures were shorter than the laser wavelength, and the interspaces depend on fluence for Mo and W with a 160 fs laser pulse. This phenomenon is well explained by the parametric decay model proposed by Sakabe *et al*.

Introduction

Ablation threshold of metals have been investigated experimentally and theoretically since the 1990s with respect to the mechanism of femtosecond laser ablation. Three ablation thresholds have been identified for metals irradiated with a laser pulse of $\leq$ 400 fs at a wavelength of 800 nm [1][2]. Two of the thresholds are characterized by the electronic thermal conduction length ($l \sim$ 80 nm) and optical penetration length ($\delta \sim$ 10 nm), respectively. The ablation rates at these thresholds are well expressed by the two-temperature thermal diffusion model. However, the third (low) ablation threshold can not be characterized by this model because the ablation rate is ~0.01 nm/pulse (less than one atomic layer) and the threshold is strongly dependent on laser pulse duration. The ablation rates are well explained by the assumption of multiphoton absorption [3]. We defined this region in which characterized by the low ablation threshold as " nano-ablation". As a result of the nano-ablation, high energy singly charged ions are emitted from metal surface and periodic grating structure is self-formed on metal surface. In this paper, the mechanism of the nano-ablation for metals is reviewed and the current study for simulation of the nano-ablation is also introduced.

1.1 Energetic ion emission from metals in femtosecond laser nano-ablation.

In order to elucidate the dynamics of the ejected particles, the velocity distribution of ions emitted from the metal by femtosecond laser ablation has been measured by time-of-flight (TOF) mass spectrometry. However, the observations were limited to a laser intensity of one order of magnitude higher than the low ablation threshold since less than one ion is ejected near the threshold per pulse. Therefore, the velocity distribution could not be obtained by single-pulse laser irradiation. With regard to the laser intensity at the low ablation threshold, the absence of collisional and Coulomb effects or chemical reactions in the ablation plume are expected. Thus, the TOF velocity distribution reflects the surface dynamics of ion ejection. In the experiment, femtosecond laser ablation of Cu by using T^6-laser system (800 nm, 130 fs)[4] was studied with TOF mass spectrometry (Jordan D-850)[5] in the laser energy fluence range of 0.028 - 14.4 J/cm^2.

1.2 How to produce the ions on metal surface

Three thresholds for ion emission were identified as shown in Fig.1. The number of emitted ions per laser pulse N_i was dependent on laser fluence and was in good agreement with $N_i \propto F^4$ for laser fluence of $F_{th,L}$ - $F_{th,M}$, $N_i \propto F^3$ for laser fluence of $F_{th,M}$ -$F_{th,H}$, and $N_i \propto F^2$ for $\geq F_{th,H}$[3]. The process of ion production is well explained by multi-photon absorption and optical field effects. Cu particles were ejected by m-photon absorption while Cu ions depended on F^{m+1} as discussed in later. The ionization potential of Cu is 6.66 eV,

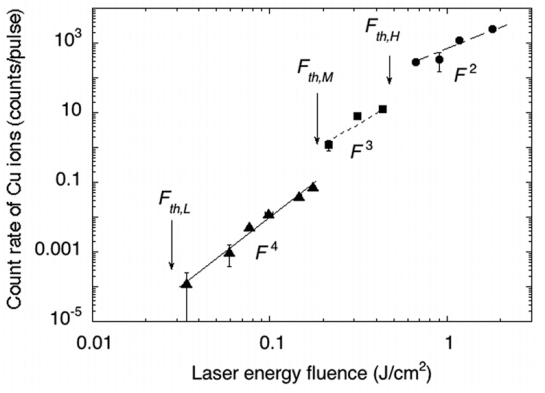

Figure 1: Number of detected Cu ions as a function of laser energy fluence.

and its work function is 4.65 eV. Therefore, at least five photons are necessary to ionize a Cu atom with an 800 nm laser (= 1.5499 eV) and four photons are necessary for multiphoton electron ejection from a Cu surface. These simple considerations do not adequately explain the observed ion production with a dependence of F^{m+1} over a wide fluence range. These experimental results suggest that the Cu ions are produced by the optical field ionization via multiphoton absorption at the sample surface. When a high-intensity laser is used to irradiate the sample surface, the bound potential of free electrons is distorted by the electric field of the laser parallel to the surface normal. This distortion of potential induces tunneling photoelectron ejection from the metal surface via multiphoton absorption. Keldysh has shown the tunneling criterion for the possibility of ejecting an electron that has bounded potential [6],

$$\gamma = \frac{\nu_L \sqrt{2m_e W}}{eE} \le 1, \qquad (1)$$

where γ is the Keldysh parameter, ν_L is the laser frequency, m_e is the mass of an electron, W is the work function at room temperature, E is the amplitude of a laser electric field, and e is the electronic charge. For an electron that absorbed m photons, the work function can be reduced to $W - mh\nu_L$; therefore, γ can be written as,

$$\gamma_m = \frac{\nu_L \sqrt{2m_e (W - mh\nu_L)}}{eE} \le 1, \qquad (2)$$

where $\nu_L = 3.75\times10^{14}\ s^{-1}$, $m_e = 9.109\times10^{-31}$ kg, $W = 7.449\times10^{-19}$ J (for Cu), $e = 1.602\times10^{-19}$ C, $E = 1.27\times10^{9}$ V/m for $F_{th,L} = 0.028$ J/cm^2, 3.36×10^{9} V/m for $F_{th,M} = 0.195$ J/cm^2, and 5.21×10^{9} V/m for $F_{th,H} = 0.470$ J/cm^2. Under the ion emission thresholds, the tunneling criterion is satisfied as γ_3=0.013 for three photons, γ_2=0.47 for two photons, and γ_1=0.43 for one photon. For all m-photon absorptions, it is possible to eject an electron by the tunneling process shown in Fig. 2

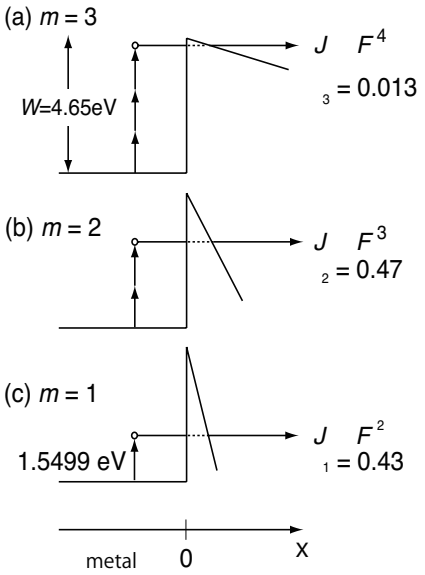

Figure 2(a)-(c) : Intense laser irradiation can ionize metal instanta neously by the optical field ionization via multiphoton absorption and produce metal ions. Vertical and horizontal axes show the energy level of a free electron and space x, respectively. x=0 shows the interface between the metal and vacuum. The energy level on the vacuum side is distorted by the electric field of the laser perpendicular to the surface. The distortion of the energy level (triangle shape) induces photoelectron ejection via tunneling. γ_m is the Keldysh parameter under the m-photon absorption modified by authors. Under the ion emission thresholds, the tunneling criterion is satisfied as γ_3 =0.013 for three photons, γ_2=0.47 for two photons, and γ_1=0.43 for one photon[3].

and produce ions on the surface. Thus, the number of ions produced is equal to the number of electrons ejected. In order to estimate the current density of ejected electrons, the Flower-Nordheim (F-N) model was used. The current density of electrons from a material under an electric field applied to the surface normal can be expressed as

$$J = \frac{A\beta^2 E^2}{\phi} \exp\left(\frac{B\phi^{2/3}}{\beta E}\right) \propto E^2, \quad (3)$$

where $A = 1.5\times10^{-6}$, $B = 6.83\times10^{9}$, β is the field enhancement factor, ϕ is the bound potential, and E is the applied electric field. In the present experiment, the laser was focused at an incident angle of 70 degrees relative to the Cu surface, and the corresponding electric field of the laser was ~ 10^9 -10^{10} V/m. In an electric field of this strength, the exponential term in Eq. (3) is ~1. Therefore, the current density of ejected electrons is proportional to laser energy fluence: $J \propto F = E^2$. Therefore, during tunneling photoelectron ejection from a metal surface with multiphoton absorption, ion production is expected to be dependent on F^{m+1}. High-energy Cu ions of 30 eV were produced at a

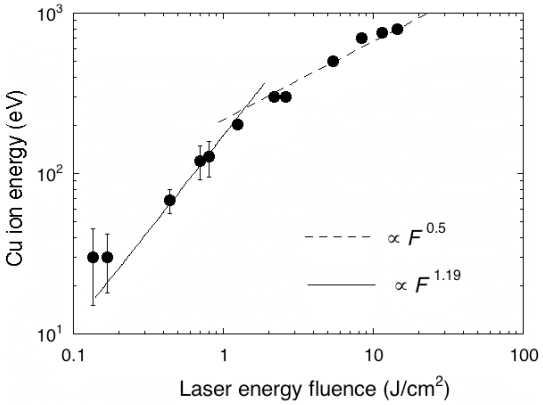

Figure 3: Dependence of most probable energy of Cu ions on laser energy fluence.

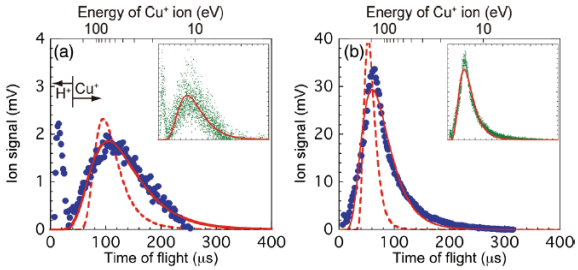

Figure 4: The TOF spectra for copper irradiated by femtosecond laser pulse(F=80mJ/cm^2, 170fs, 800nm) . (a) Copper surface with mechanically polished and (b) Structured surface structure on copper with femtosecond laser pre-irradiation. Dashed lines and solid lines indicate the calculated SMB distribution and CEN distribution, respectively.

low laser fluence of 0.136 J/cm^2. The most probable energy of Cu ions increased as the laser energy fluence increased as shown in Fig. 3. In this report, we classify the laser fluence into three ion emission regimes (see Fig. 1). The number of emitted ion per laser pulse N_i was dependent on laser fluence and in good agreement with $N_i \propto F^4$ for low fluence (F = 0.028 - 0.195 J/cm^2), $N_i \propto F^3$ for medium fluence (F = 0.195 - 0.47 J/cm^2) and $N_i \propto F^2$ for high fluence ($F \geq$ 0.47 J/cm^2). The process of ion production is well explained by multiphoton absorption and optical field ionization. The interesting Cu ion energy in the fluence range of 0.10 - 1.2 J/cm^2 is shown in Fig. 3. Thus, we discuss the ion energy not only at low laser fluence but also at medium and high laser fluence. In the fluence range of 0.10 - 1.2 J/cm^2, the energy of Cu ions is proportional to the laser fluence, $E \propto F^{1.19}$. This relation was analyzed within the framework of the Coulomb explosion of ions that were localized to the metal surface, and could satisfactorily and qualitatively explain the obtained results as mentioned in [3]. In the case of non-thermal ablation, the formation of grating structures on the Cu surface has been observed in this fluence range [7], and the interspaces of these grating structures are much shorter than the thermal diffusion length. Therefore, the formation of grating structures would not be observed if thermal ablation were the dominant process. On the other hand, the dependence of Cu ion energy on laser fluence was investigated for laser fluence greater than 1.2 J/cm^2; the relation was observed experimentally to be $E \propto F^{0.5}$. This result is well explained by the emission of ions under thermal equilibrium conditions, where the most probable energy is related to the laser fluence as $E_{PEAK} \propto F^{0.5}$. This is in reasonable agreement with the experimental results. Thus, the ions might be produced by thermal ablation for laser fluence greater than 1.2 J/cm^2. For thermal ablation at fluence greater than 1.2 J/cm^2, the formation of grating structures on the Cu surface has not been observed [7]. Therefore, the energy of the emitted ions indicates that Cu is ablated by a thermal process only for laser fluence greater than 1.2 J/cm^2, while a non-thermal process (Coulomb explosion) is operative in the fluence range of 0.1 - 1.2 J/cm^2. In Fig. 3, the ion energy is shown, excluding ion energies for fluence greater than 1.2 J/cm^2, and the fluence dependence is discussed in terms of the Coulomb explosion of Cu ions produced by a multiphoton process and optical field ionization.

The experimental results were analyzed within the framework of the Coulomb explosion of ions that were localized to the metal surface, which could satisfactorily and qualitatively explain the obtained results[3][8].

1.3 Energy distribution function of emitted metal ions

Figure 4 shows the TOF spectrum of emitted ions for femtosecond laser pulse irradiation on copper. The ion spectra have a double-peak structure. The fast and slow components correspond to protons and singly charged copper ions, respectively. In Fig.4(a), the TOF spectrum for the nanoparticles distributed on copper surface is shown. The size distribution of nanoparticles was lognormal, a mean radius r_c was 7.7nm, and the standard deviation of the logarithmic radius w was 0.41. The dashed line shows a least squares fit of a sifted Maxwell-Boltzmann (SMB) distribution in which is well used for thermal ablation. The TOF spectrum could not be fitted with the SMB distribution. The solid line shows calculation with a Coulomb explosion of nanopartices (CEN) in which we have proposed recently [9]. This CEN model is expressed as

$$f(t) = \frac{C}{t^3}\exp\left[-\frac{1}{2w^2}\left\{\ln\left(\frac{L\sqrt{3\varepsilon_0 m_i/(2ne^2)}}{tr_c\sqrt{i}}\right)\right\}^2\right], \quad (4)$$

where C is a distribution normalization constant, L is a flight distance for TOF measurement, w is the standard deviation of the logarithmic radius, ε_0 is

the vacuum permittivity, m_i is the mass of metallic element, n is the atomic density in nanoparticle, e is the electronic charge, i is the ionization rate in nanoparticle, t is the flight time of metal ion, and r_c is the mean radius of nanoparticles. In the calculation, L =1.45m, w=0.41, ε_0=8.85×10^{-12} F/m, m_i=1.05×10^{-25} kg, n= 8.85×10^{28} m^{-3} for copper, e =1.60×10^{-19} C, and r_c =7.7 nm are used. The least square fit of Eq.(4) to TOF spectrum give us the i=0.072%.

In Fig. 4(b), the TOF spectrum for laser produced structures (different morphology from that for Fig. 4(a)) on copper surface is shown. The surface structure was produced by femtosecond laser pre-irradiation and measured by using a field-emission scanning electron microscopy (FE-SEM). In this case, the ion emission is more enhanced and the peak energy was sifted toward higher side. With using the i=0.072%, TOF spectrum in Fig.4(b) is well fitted with the calculation of CEN model as shown in solid line. In the calculation r_c=13nm and w=0.42 are used. The presence of larger nanoparticles (r_c~13nm) on metals surface was shown by FE-SEM observation.

In nano-ablation for metal, the emission of the energetic ions non-thermally occurred through the nanoparticles interacted with femtosecond laser pulses. We confirmed that the Ion energy distribution was expressed by the calculation with a Coulomb explosion of nanopartices.

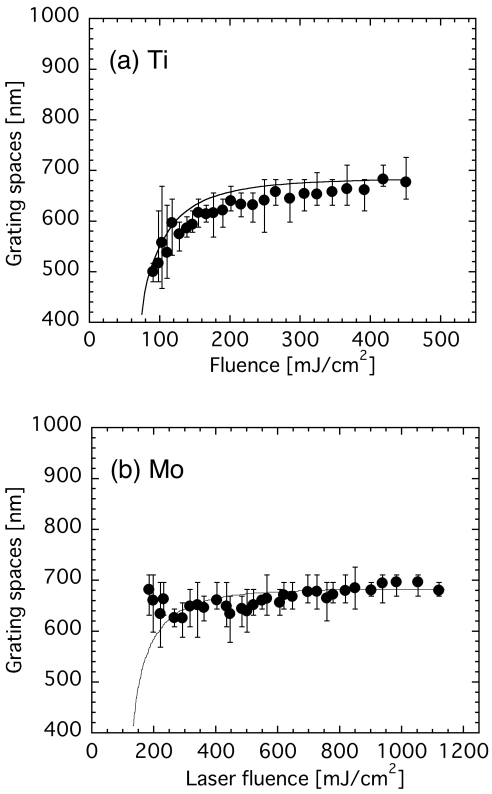

Figure 5: Laser fluence dependence of the periodic structure interspaces produced by femtosecond laser pulses (pulse duration: 160 fs at 800nm). Solid lines show calculation results based on the parametric decay model [6].

2.1 Periodic grating structures formation in femtosecond laser nano-ablation

Recently, the formation of grating structures on metal surfaces has been observed [10][11] and used in chemical application [12]. For fluence levels near the low ablation threshold, the grating structures had an interspace of 300 nm, which was much shorter than the laser wavelength of 800 nm. The interspaces of the grating structures depended on laser fluence, and this phenomenon was well explained by the parametric decay model [7] proposed by Sakabe *et al*. To confirm the validity of this model, the interspaces dependence on laser fluence for Ti, Pt, Mo, and W have been measured experimentally [13]. We found that the experimental results agreed reasonable well with this model. In this model, a femtosecond laser pulse interacts with the metal and a photon in the IR region, and a plasma wave decays along the surface. The plasma wave travels slowly at a speed of less than 10^{-2} times that of light, and an ion-enriched local area appears. Before the next electron wave peak arrives, the ions experience a strong Coulomb repulsive force and can be exploded into a vacuum; in other words, a Coulomb explosion [14] occurs. Through this process, periodic grating structures are formed. The mechanism of grating structure formation is currently under investigation. In the experiments, T^6-laser system (λ=800 nm, τ =160 fs, 10 Hz)[4] has been used. The laser beam is focused to a spot size of φ 45 μm on the target surface with a lens (f = 10 cm), at normal incidence in air. To avoid nonuniformity of intensity in the irradiated area on the surface, the laser intensity distribution is adjusted to be spatially uniform. The targets are Ti and Mo metals, which are mechanically polished. The roughness, R_a, is less than 2 nm for metals. The fluence is varied in the range of F = 50 - 2100 mJ/cm^2. The number of irradiating pulses is 50. Laser-produced surface structures are examined by scanning electron microscopy (JSM-5560, JEOL). The periodic grating interspace is determined by reading the peak value in the frequency domain after taking the Fourier transform for the 20 μm × 15 μm area of the SEM image, which is equivalent to the laser irradiated area on the targets. The resolution of the present measurements of the periodic spacing is better than 34 nm. Figure 5 shows typical dependence of the periodic structure interspaces on laser fluence for Ti and Mo metals. Solid lines show calculation results according to the parametric decay model, in which ablation threshold is taken into account. As shown in Fig. 5, the model is in good agreement with the experimental results in the fluence range in which periodic grating structures are formed. These experimental results indicate that the formation

threshold of grating structure is closely related to ablation threshold.

Here, the parametric model is briefly described. The parametric process of photon → photon + plasmon can occur on a plasma surface as well as in a bulk plasma (i.e., stimulated Raman scattering). The parametric conditions of $\omega_L = \omega_2 + \omega_{SP}$ and $\mathbf{k}_L = \mathbf{k}_2 + \mathbf{k}_{SP}$, where the subscripts L, 2, and SP indicate the incident laser light, scattered light, and surface plasma wave, respectively, are reduced to

$$\omega_L - \omega_{SP} = ck_{SP} - ck_L,\ \omega_L = ck_L,$$

$$\omega_{SP}^{\ 2} = c^2 k_{SP}^{\ 2} + \frac{1}{2}\omega_p^{\ 2} - \left(c^4 k_{SP}^{\ 4} + \frac{1}{4}\omega_p^{\ 2}\right)^{1/2}.$$

The wavenumber of the plasma wave induced by the parametric process can be related to the plasma frequency, and the k_L/k_{SP} ratio (= λ_{SP}/λ_L; λ is the wavelength) changes from 0.5 to 0.85 for plasma frequencies in the range of $0 < \omega_p/\sqrt{2} < \omega_L$, where the plasma wavenumber increases as the plasma frequency decreases. As mentioned above, assuming that the self-formation is induced by the plasma wave, the grating spaces correspond to the wavelength of the induced plasma wave, and the fluence dependence of the interspaces can be reduced to plasma density dependence. The dependence of the surface electron density n_{es} on the laser fluence F_L can be interpreted as follows. The electron density n_e of the bulk plasma produced on the surface by the laser is related to the ablation threshold F_{th}: $n_e \propto \ln(F_L/F_{th})$. The threshold F_{th} for Ti was 74 mJ/cm^2 and for Mo was 134 mJ/cm^2 under 800-nm pulses [13]. A reasonable assumption is that plasma formation starts at the ablation threshold F_{th} [15]. The heated plasma bulk with temperature T_e expands at the sonic speed $c_s=(k_B T_e/m_e)^{1/2}$, and the surface electron density decreases from the bulk density as n_e/c_s, and the temperature is proportional to the laser energy: $T_e \propto F_L$. Therefore, the surface electron density is related to the laser fluence as $n_{es} \propto n_e/c_s \propto n_e/T^{1/2} \propto \ln(F_L/F_{th})/F_L^{1/2}$. It is reasonable to assume that the plasma frequency is $\omega_p = \sqrt{2}\omega_L$ for the laser fluence F_M since no grating structures are produced at laser fluence over F_M. Thus we can clearly see the upper limit F_M on laser fluence for producing periodic structures. In this case, $n_{es}[\mathrm{cm}^{-3}]=3.5\times10^{21}\ln(F_L/F_{th})/F_L^{1/2}$. Applying this expression together with $\omega_P=(4\pi n_{es}e^2/m_e)^{1/2}$ to the dependence of λ_{SP}/λ_L on ω_P, the spatial dependence of the laser fluence is obtained. This relation is shown as a solid line in Fig. 5. For each metal, the experimental results agree reasonably well with this model.

2.2 PIC simulation for periodic grating structures formation.

The surface plasma wave induced by femtosecond laser is key issue to discuss the mechanism of the periodic grating structures. However, the surface plasma wave could not observe directly due to experimental difficulties. Thus the formation of periodic structures is not yet fully understood. In this section, we introduced the recent results to visualize the surface plasma wave with two dimensional particle in cell (2D-PIC) simulation.
In order to visualize the surface plasma wave induced by femtosecond laser, two-dimensional particle in cell simulation by using the code FISCOF[16] has been demonstrated for initially pre-formed plasma on a target. For the simulation, the pre-formed plasma has the thickness of 2 μm in the x direction of the (x, y) simulation plane. The electron density of the pre-plasma was varied in the range of 0 - n_{ct} by 0.1n_{ct} step, where n_{ct} was the critical density for 800nm wavelength. The plasma was initially characterized by a Maxwellian distribution with electron temperature T_e=1 keV

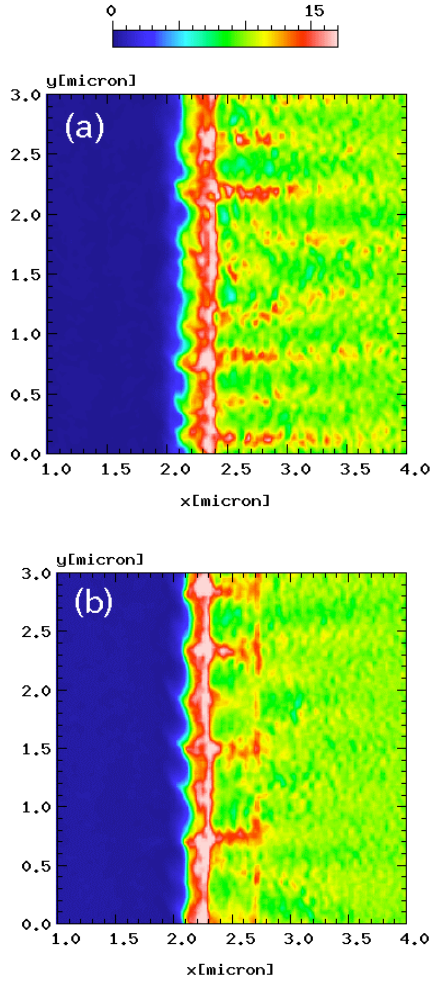

Figure 6: The electron density profiles in the x-y plane at t=220 [fs] in case of the thin plasma density of (a) 0.3n_{ct} and (b) 0.7n_{ct}[17]. Electron density is normalized by n_{ct}.

and ion temperature $T_i = 0.1T_e$. Hydrogen plasma $m_i / m_e = 1836$ is used, where m_i and m_e are the ion and electron mass. The charge of the ions is $Z = 1$. The target of 10 n_{ct} was located behind the pre-plasma and its dimension of 10 μm thick and 8 mm wide. Intense laser ($I=1.56\times10^{18}$ W/cm^2, λ=800 nm, rise time =15 fs) was irradiated continuously onto the preformed plasma target with normal incidence. The laser was linearly polarized with the direction parallel to y axis. Figure 6 shows the electron density distribution at the t = 220 fs for $0.3n_{ct}$ and $0.7n_{ct}$ of pre-plasma. The simulation results show that the surface wave is produced on the pre-plasma surface at x = 2.0 μm. The period of the surface wave was analyzed by 1D Fourier transform for the electron density distribution in y direction. Before the analyzation, the electron density is integrated along the x direction from 1.8 to 2.5μm. The period of surface wave is ~ 480 nm at 0.7 n_{ct} and depend on pre-plasma density n_{ct}. The obtained simulation result is helpful to discuss the dynamics of the surface plasma wave generation. However, the irradiated laser intensity is set 4 order of magnitude higher than that obtained by the experiment since the multi pulse irradiation effect could not take it into account for this 2D-simulation in realistic calculation time. The nano grating structure was self-formed experimentally as a result of multi pulse irradiation in the range of 50 - 10,000 pulses. To reduce this discrepancy, we need further investigation to express as a cumulation effect for multi pulse irradiation.

Conclusions

In summary, we have introduced recent results for ion emission from metals surface and periodic structures self-formed on metals to discuss the dynamics of nano-ablation for metals. The process of ion production is well explained by multiphoton absorption and optical field ionization. The experimental observations are self-consistent with the interpretation that the ions are emitted by Coulomb explosion of ions localized on the metal surface by an intense femtosecond laser pulse. This ion emission might be contributed to produce surface pre-plasma on metals. Therefore, low dense pre-plasma is formed on metal surface before peak intensity of laser is reached. We believed that the periodic grating structure is self-formed on metals, since the initial condition for parametric decay process is fulfilled. Our proposed model still includes several assumptions, therefore, we need further investigations to discuss more detailed.

Acknowledgments

This study was financially supported by a Grant-in-Aid for Scientific Research (C)(22560720) from the Ministry of Education, Culture, Sports, Science and Technology (MEXT), Japan, the Research Foundation of the Murata Science Foundation, and the Amada Foundation for Metal Work Technology, NIFS Collaborative Research Program (NIFS11KNTS013) and was partially supported by the Grant-in-Aid for the Global COE Program "The Next Generation of Physics, Spun from Universality and Emergence" from the Ministry of Education, Culture, Sports, Science and Technology (MEXT) of Japan. This work is performed with the support

References

[1] M. Hashida, A. Semerok, O. Govert, G. Petite, and J. F-. Wagner (2000) Ablation thresholds of metals with femtosecond laser pulses, in Proc. SPIE 4423, pp.178-185.

[2] M. Hashida, A. Semerok, O. Govert, G. Petite, Y. Izawa, and J. F-. Wagner (2002), Ablation threshold dependence on pulse duration for copper, Applied Surface Science, 197-198, 862-867.

[3] M. Hashida, S. Namba, K. Okamuro, S. Tokita, S. Sakabe (2010), Ion emission from a metal surface through a multiphoton process and optical filed ionization, Physical Review B, 81, 115442.

[4] S. Tokita, M. Hashida, S. Masuno, S. Namba, and S. Sakabe (2008), 0.3% energy stability, 100 milijoule-class, Ti:sapphire chirped-pulse eight-pass amplification system, Optics Express 16, 14875-14881.

[5] J. Kou, V. Zhakhovskii, S. Sakabe, K. Nishihara, S. Shimizu, S. Kawato, M. Hashida, K. Shimizu, S. Bulanov, Y. Izawa, Y. Kato, N. Nakashima (2000), Anisotropic Coulomb explosion of C_{60} irradiated with a high-intensity femtosecond laser pulse, Journal of Chemical Physics, 112, 5012-5020.

[6] L. V. Keldysh (1965), Ionization in the field of a strong electromagnetic wave, Soviet Physics JETP, 20, 1307-1314.

[7] S. Sakabe, M. Hashida, S. Tokita, S. Namba, K. Okamuro (2009), Mechanism for self-formation of periodic grating structures on a metal surface by a femtosecond laser pulse, Physical Review B, 79, 033409.

[8] M. Hashida, Y. Miyasaka, Y. Ikuta, S. Tokita, and S. Sakabe (2011), Crystal structures on a copper thin film with a surface of periodic self-organized nanostructures induced by femtosecond laser pulses, Physical Review B, 83, 235413-1-235413-5.

[9] Y. Miyasaka, M. Hashida, Y. Ikuta, K. Otani, S. Tokita, and S. Sakabe (2012), Nonthernmal emission of energetic ions from a metal surface irradiated by extremely low-fluence femtosecond laser pulses, Physical Review B 86, 075431.

[10] M. Hashida, M. Fujita, M. Tsukamoto, A. Semerok, O. Govert, G. Petite, Y. Izawa, and J. F-. Wagner (2003), Femtosecond laser ablation of metals: precise measurement and analytical model

for crater profiles, in Proc. SPIE 4830, pp.452-457.
[11] M. Tsukamoto, K. Asuka, H. Nakano, M. Hashida, M. Katto, N. Abe, M. Fujita (2006), Periodic microstructure produced by femtosecond laser irradiation on titanium plate, Vacuum, 80, 1346-1350.
[12] S. Matsumoto, A. Yane, S. Nakashima, M. Hashida, M. Fujita, Y. Goto, and S. Takahashi (2007) , A rapid flow mixer with 11-μs mixing time microfabricated by a pulsed laser ablation technique: observation of a barrier-limited collapse in cytochrome *c* folding, Journal of the American Chemical Society, 129, 3840-3841.
[13] K. Okamuro, M. Hashida, Y. Miyasaka, Y. Ikuta, S. Tokita, and S. Sakabe (2010), Laser fluence dependence of periodic grating structures formed on metal surfaces under femtosecond laser pulse irradiation, Physical Review B, 82, 165417.
[14] S. Sakabe, K. Shirai, M. Hashida, S. Shimizu, and S. Masuno (2006), Skinning of argon clusters by Coulomb explosion induced with am intense femtosecond laser pulse, Physical Review A, 74, 043205.
[15] P. P. Pronko, S. K. Dutta, D. Du, and R. K. Singh (1995), Thermophysical effects in laser processing of materials with picosecond and femtosecond pulses, Journal of Applied Physics, 78, 6233-6240.
[16] H. Sakagami and K. Mima (2002), Fast ignition simulations with collective PIC code, Proc. 2nd Int. Conf. Inertial Fusion Sci. Appl., Kyoto, 2001, pp380-383.
[17] T. Ogata, H. Sakagami, M. Hashida, and S. Sakabe (2012), PIC simulations for periodic nano-grating structures induced by femtosecond laser pulse, Proceedings of LPM2012, No.20, pp.1-4.